

RESEARCH PAPER



Discovery of novel mRNA demethylase FTO inhibitors against esophageal cancer

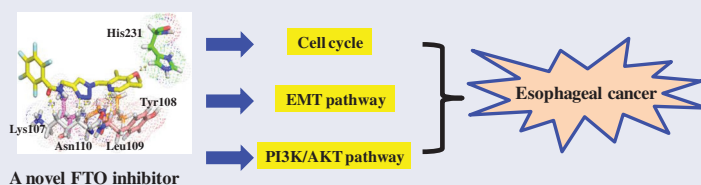
Bo Qin^{a*}, Qian Bai^{b*}, Dan Yan^a, Fanxiang Yin^a, Zhu Zhu^a, Chaoyuan Xia^a, Yang Yang^a and Yi Zhao^a

^aTranslational Medical Center, The First Affiliated Hospital of Zhengzhou University, Zhengzhou, PR China; ^bDepartment of Anesthesiology, The Second Affiliated Hospital of Zhengzhou University, Zhengzhou, PR China

ABSTRACT

A series of 1,2,3-triazole analogues as novel fat mass and obesity-associated protein (FTO) inhibitors were synthesised in this study. Among all 1,2,3-triazoles, compound **C6** exhibited the most robust inhibition of FTO with an IC₅₀ value of 780 nM. It displayed the potent antiproliferative activity against KYSE-150, KYSE-270, TE-1, KYSE-510, and EC109 cell lines with IC₅₀ value of 2.17, 1.35, 0.95, 4.15, and 0.83 μM, respectively. In addition, **C6** arrested the cell cycle at G2 phase against TE-1 and EC109 cells in a concentration-dependent manner. Analysis of cellular mechanisms demonstrated that **C6** concentration-dependently regulated epithelial mesenchymal transition (EMT) pathway and PI3K/AKT pathway against TE-1 and EC109 cells. Molecular docking studies that **C6** formed important hydrogen-bond interaction with Lys107, Asn110, Tyr108, and Leu109 of FTO. These findings suggested that **C6** as a novel FTO inhibitor and orally antitumor agent deserves further investigation to treat esophageal cancer.

GRAPHICAL ABSTRACT



ARTICLE HISTORY

Received 6 May 2022
Revised 30 June 2022
Accepted 3 July 2022

KEYWORDS

FTO; 1,2,3-triazole;
esophageal cancer; cell
cycle; molecular docking



1. Introduction

Esophageal cancer as the eighth most common cancer in the world possesses the poor prognosis and poor survival¹. It is necessary to develop effective and novel drugs to treat esophageal cancer². Fat mass and obesity-associated protein (FTO), a demethylase for N⁶-methyladenosine modification, has been implicated in esophageal cancer³. Recent report demonstrated that esophageal cancer tissues had the increased FTO expression which correlated with clinical esophageal cancer prognosis⁴. In addition, FTO could play oncogenic roles and promote cell proliferation and migration in esophageal cancer⁵. Therefore, FTO might be a potential target and FTO inhibitors might be effective and novel anticancer agents for the treatment of esophageal cancer.

1,2,3-Triazole as one of the most important classes of nitrogen-containing heterocycle exhibits potent anticancer activity⁶. 1,2,3-triazole-benzoxazole hybrid **1** (Figure 1) displayed antiproliferative activity against SKBr3, HepG2, and HeLa cells with IC₅₀ values of 7.1, 11.2, and 6.8 μg/mL⁷. 1,2,3-Triazole-benzisoxazole hybrid **2** showed antiproliferative activity against MOLM13, MOLM14, and MV4-11 cell lines⁸. Hybrid **3** inhibited migration and mammosphere formation and

induced cell cycle arrest at G2-M phase against breast cancer cells⁹. On the other hand, pyridine derivatives also have a wide-range of therapeutic applications in the area of drug discovery¹⁰. Pyridine analogue FTO-IN-5 (Figure 1) as a selective FTO inhibitor could decrease the viability of acute monocytic leukaemia cells and increase the level of N⁶-methyladenosine in mRNA¹¹. Pyridine analogue FTO-IN-6 selectively inhibited FTO and formed hydrogen bonds with residues Ser318 and Tyr295¹².

Molecular hybridisation, involving a combination of two or more bioactive scaffolds to generate a single molecular architecture, has been a promising strategy in the drug discovery research¹³. Furthermore, fluorine as the most electronegative element plays a key role to design anticancer agents¹⁴. Therefore, a class of 1,2,3-triazole-pyridine hybrids containing a pentafluorobenzoyl moiety as potential FTO inhibitors was designed by the molecular hybridisation. In addition, these compounds were evaluated for their anticancer activity *in vitro* and *in vivo* against esophageal cancer cell lines. To the best of our knowledge, it is the first time to discover that 1,2,3-triazole-pyridine hybrids could be potential anticancer agents by targeting FTO for the treatment of esophageal cancer.

CONTACT Bo Qin  boqin@mail.ustc.edu.cn; Yang Yang  yangyangbio@163.com; Yi Zhao  zhaoyi0910@163.com  Translational Medical Center, The First Affiliated Hospital of Zhengzhou University, No.1 Eastern Jianshe Road, Zhengzhou, PR China

*These authors contributed equally to this work.

 Supplemental data for this article is available online at <https://doi.org/10.1080/14756366.2022.2098954>.

© 2022 The Author(s). Published by Informa UK Limited, trading as Taylor & Francis Group.

This is an Open Access article distributed under the terms of the Creative Commons Attribution License (<http://creativecommons.org/licenses/by/4.0/>), which permits unrestricted use, distribution, and reproduction in any medium, provided the original work is properly cited.

64.82, 64.48, 52.43, 34.90, 9.70. HR-MS (ESI): calcd for $C_{19}H_{14}F_8N_5O_2$, $[M + H]^+$ 496.1020; found: 496.1025. Purity: 97.43%.

2.3.7. 2,3,4,5,6-Pentafluoro-N-((1-((4-methoxy-3,5-dimethylpyridin-2-yl)methyl)-1H-1,2,3-triazol-4-yl)methyl)benzamide (C6)

White solid, yield: 62%. Mp: 135–137 °C. 1H NMR (400 MHz, DMSO- d_6) δ 9.44 (t, $J = 5.3$ Hz, 1H), 8.18 (s, 1H), 7.90 (s, 1H), 5.69 (s, 2H), 4.53 (d, $J = 5.6$ Hz, 2H), 3.73 (s, 3H), 2.23 (d, $J = 19.3$ Hz, 6H). ^{13}C NMR (100 MHz, DMSO- d_6) δ 163.57, 156.54, 152.66, 148.99, 143.45, 125.78, 124.66, 123.48, 59.79, 52.57, 34.91, 12.87, 10.39. HR-MS (ESI): calcd for $C_{19}H_{17}F_5N_5O_2$, $[M + H]^+$ 442.1302; found: 442.1307. Purity: 99.53%.

2.3.8. N-((1-((6-chloropyridin-2-yl)methyl)-1H-1,2,3-triazol-4-yl)methyl)-2,3,4,5,6-pentafluorobenzamide (C7)

White solid, yield: 88%. Mp: 148–150 °C. 1H NMR (400 MHz, DMSO- d_6) δ 9.44 (t, $J = 5.3$ Hz, 1H), 8.45 (d, $J = 2.3$ Hz, 1H), 8.14 (s, 1H), 7.81 (dd, $J = 8.3, 2.5$ Hz, 1H), 7.55 (d, $J = 8.2$ Hz, 1H), 5.69 (s, 2H), 4.54 (d, $J = 5.5$ Hz, 2H). ^{13}C NMR (100 MHz, DMSO- d_6) δ 156.55, 150.09, 149.47, 144.01, 139.55, 131.34, 124.39, 123.33, 49.38, 34.88. HR-MS (ESI): calcd for $C_{16}H_{10}ClF_5N_5O$, $[M + H]^+$ 418.0494; found: 418.0497. Purity: 98.24%.

2.3.9. N-((1-((1H-benzo[d]imidazol-2-yl)methyl)-1H-1,2,3-triazol-4-yl)methyl)-2,3,4,5,6-pentafluorobenzamide (C8)

White solid, yield: 73%. Mp: 232–234 °C. 1H NMR (400 MHz, DMSO- d_6) δ 12.68 (s, 1H), 9.46 (t, $J = 5.4$ Hz, 1H), 8.13 (s, 1H), 7.55 (dd, $J = 35.7, 7.6$ Hz, 2H), 7.34–6.97 (m, 2H), 5.88 (s, 2H), 4.57 (d, $J = 5.6$ Hz, 2H). ^{13}C NMR (100 MHz, DMSO- d_6) δ 156.59, 148.24, 143.84, 123.66, 47.24, 34.89. HR-MS (ESI): calcd for $C_{18}H_{12}F_5N_6O$, $[M + H]^+$ 423.0993; found: 423.0998. Purity: 98.15%.

2.4. In vitro enzymatic activity against FTO

Of 50 μ L of buffer solution containing 2 mM L-ascorbic acid, 2 nM FTO, 2 M ssRNA, 280 μ M $(NH_4)_2Fe(SO_4)_2$, 1 mM α -KG, and 50 mM Tris-HCl was prepared to perform the enzymatic reaction. Compounds with different concentrations were added into the solution and incubated at room temperature for 30 min. Then, the enzymatic reaction was quenched by heating at 95 °C for 5 min. ssRNA, nuclease P1, NH_4OAc , NH_4HCO_3 , and alkaline phosphatase were added and incubated at 37 °C for 3 h. Finally, the nucleosides were separated and detected using a Thermo TSQ Quantum Ultra LC/MS (Thermo Fisher Scientific, Waltham, America). Concentration-response curves were fitted with GraphPad Prism version 6.0 (GraphPad Software, San Diego, CA).

2.5. Cell proliferation assay

KYSE-150, KYSE-270, TE-1, KYSE-510, and EC109 cell lines were purchased from Shanghai Yuanye Biotechnology Co., LTD (Shanghai, China). EC109&shFTO and EC109&shControl cell lines were supported by Servicebio (Wuhan, China). All these cells were maintained in RPMI-1640 medium (Shanghai Yuanye Biotechnology Co., LTD, Shanghai, China) with 10% foetal bovine serum (Shanghai Yuanye Biotechnology Co., LTD, Shanghai, China) and 1% penicillin-streptomycin in a humidified atmosphere of 5% CO_2 at 37 °C. Cells were cultured with compounds at different concentrations for 72 h. Next, 5 mg/mL MTT (Servicebio, Wuhan, China) was added and incubated for 4 h. DMSO was added into the

system and shocked for 10 min. The absorbance at 490 nm was measured by using a multifunction microplate reader (Thermo Fisher Scientific, Waltham, MA).

2.6. Western blotting

RIPA buffer solution (Servicebio, Wuhan, China) was used to perform western blot. Of 20 μ L of protein solution were subjected to SDS-PAGE, and then transferred to nitrocellulose membranes (Shanghai Yuanye Biotechnology Co., LTD, Shanghai, China). Of 5% non-fat milk (Servicebio, Wuhan, China) was used to block the system and nitrocellulose membranes were incubated at 4 °C with the first antibody overnight, followed by the incubation with a secondary antibody. Finally, blots were visualised by the chemiluminescence kit (Shanghai Yuanye Biotechnology Co., LTD, Shanghai, China).

2.7. Molecular docking studies

Studies of molecular modelling in this work were performed with Autodock software (The Scripps Research Institute, San Diego, CA). The crystal structure of FTO (PDB code: 5DAB) was downloaded from the RCSB protein database (<http://www.rcsb.org/>). Hydrogen-bond interaction between FTO and compounds was analysed by Pymol software (DeLano Scientific LLC, San Carlos, CA).

2.8. Cell cycle arrest

Cells were incubated with the targeted compound at different concentrations for 48 h and harvested. Of 70% cold ethanol was added and incubated at 4 °C for 12 h. Then, fixed cells were washed with PBS (Servicebio, Wuhan, China). Finally, the system was stained with PI (Servicebio, Wuhan, China) for 30 min under the dark condition and analysed by a Flow cytometer (Annoron, Beijing, China).

2.9. Xenograft study

BALB/c nude mice purchased from Shanghai Yuanye Biotechnology Co., LTD (Shanghai, China). All the animal experiments were performed according to approved guidelines from the ethics committee of Zhengzhou University (Approval number ZZU-2021-014). EC109 cell line was used to establish xenograft models in this work. Intra-gastric administration was adopted to finish the *in vivo* experiments. Organs (Heart, liver, spleen, lung, and kidney) from BALB/c mice for toxicity studies were fixed in 4% formaldehyde solution (Servicebio, Wuhan, China). Section of tissues was supported by Servicebio (Wuhan, China) and it was analysed by haematoxylin and eosin staining.

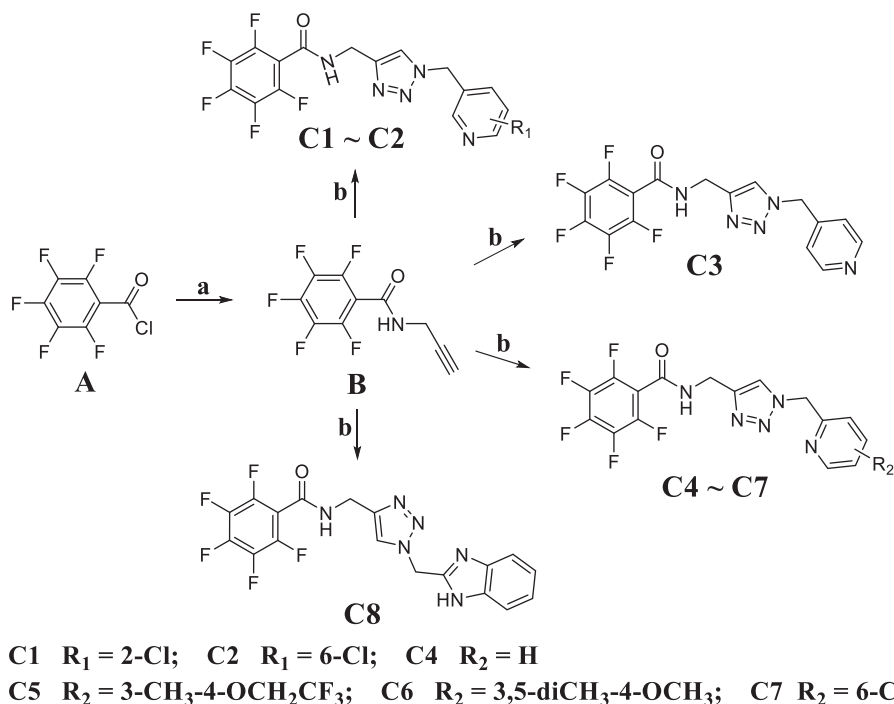
2.10. Statistical analysis

In order to maintain accuracy, each biological assay was repeated three times. In this work, $**p < 0.01$ was considered significant.

3. Results and discussion

3.1. Chemistry

Synthetic route of 1,2,3-triazole-pyridine hybrids **C1**~**C8** is displayed in Scheme 1. Intermediate **B** was obtained from the acylation reaction of prop-2-yn-1-amine with 2,3,4,5,6-



Scheme 1. Reagents and conditions: (a) prop-2-yn-1-amine, triethylamine, dichloromethane; (b) Azide derivatives, $\text{CuSO}_4 \cdot 5\text{H}_2\text{O}$, sodium ascorbate, and THF/ H_2O .

Table 1. Antiproliferative activities against esophageal cancer cell lines

Compd.	IC_{50} (μM)				
	KYSE-150	KYSE-270	TE-1	KYSE-510	EC109
B	>20	>20	>20	>20	>20
C1	11.37 ± 0.69	12.26 ± 0.80	14.33 ± 0.68	13.91 ± 0.37	18.65 ± 0.92
C2	14.60 ± 0.16	9.34 ± 0.29	10.27 ± 0.91	9.34 ± 0.21	15.22 ± 0.36
C3	10.49 ± 0.38	14.16 ± 0.90	17.31 ± 0.68	11.07 ± 0.16	6.34 ± 0.11
C4	6.55 ± 0.20	7.83 ± 0.19	9.17 ± 0.09	8.12 ± 0.72	5.29 ± 0.28
C5	4.04 ± 0.16	2.04 ± 0.57	3.09 ± 0.10	5.07 ± 0.46	3.18 ± 0.27
C6	2.17 ± 0.59	1.35 ± 0.05	0.95 ± 0.07	4.15 ± 0.13	0.83 ± 0.04
C7	6.21 ± 0.14	5.29 ± 0.20	6.19 ± 0.25	9.22 ± 0.14	5.87 ± 0.27
C8	3.59 ± 0.08	2.04 ± 0.21	1.76 ± 0.09	5.13 ± 0.17	1.66 ± 0.04
5-Fluorouracil	17.39 ± 0.21	13.05 ± 0.62	7.73 ± 0.18	13.02 ± 0.70	9.62 ± 0.35

pentafluorobenzoyl chloride in dichloromethane. Then, click reaction of intermediate **B** and appropriately substituted azide derivatives was performed to generate 1,2,3-triazole-pyridine hybrids **C1** ~ **C8** in the mixed solvent system (tetrahydrofuran: water = 1: 1).

3.2. Antiproliferative activity of compound **B** and compound **C1**~**C8** against esophageal cancer

1,2,3-Triazole-pyridine hybrids **C1**~**C8** were evaluated for their antiproliferative activities against five esophageal cancer cell lines (KYSE-150, KYSE-270, TE-1, KYSE-510, and EC109) by the MTT assay. 5-Fluorouracil (5-Fu) was employed as the reference drug in the reported reference for the antiproliferative evaluation of 1,2,3-triazole derivatives¹⁵. So, it also was used as the control to evaluate the accuracy of antiproliferative results. The antiproliferative results of compound **B** and 1,2,3-triazole-pyridine hybrids **C1**~**C8** are summarised in Table 1.

As shown in Table 1, compound **B** without the triazole-pyridine unit displayed the weak inhibitory activity against all esophageal cancer cell lines. However, 1,2,3-triazole-pyridine hybrids **C1**~**C8** with the triazole-pyridine unit exhibited inhibitory activity against all esophageal cancer cell lines with IC_{50} values

from 0.83 to 18.65 μM . These results indicated that triazole-pyridine unit might play the potential synergistic effects for inhibitory activity against esophageal cancer. Among all hybrids, compound **C6** displayed the best antiproliferative activity against KYSE-150, KYSE-270, TE-1, KYSE-510, and EC109 cell lines with IC_{50} values of 2.17, 1.35, 0.95, 4.15, and 0.83 μM , respectively.

In order to investigate the effects of substituent groups attaching to pyridine ring for the antiproliferative activity, 1,2,3-triazole-pyridine hybrids **C4**~**C7** containing different substituent groups were synthesised and evaluated. Compound **C4** displayed moderate inhibitory activity against TE-1 cell line with an IC_{50} value of 9.17 μM . Replacing the hydrogen atom with a chlorine atom (**C7**, 6.19 μM) led to a small increment of activity against TE-1 cancer cells. However, changing the 3,5-dimethyl-4-methoxy group (**C6**) to a hydrogen atom (**C4**) or a chlorine atom (**C7**) led to a decrease of activity against KYSE-150, KYSE-270, TE-1, KYSE-510, and EC109 cells. All these results illustrated that substituent groups attaching to pyridine ring played the important role for the antiproliferative activity against esophageal cancer.

Furthermore, replacing the pyridine fragment of compound **C6** with 1*H*-benzo[*d*]imidazole of compound **C8** led to a decrease of

activity against all esophageal cancer cell lines. Compound **C8** displayed the antiproliferative activity against KYSE-150, KYSE-270, TE-1, KYSE-510, and EC109 cell lines with IC_{50} values of 3.59, 2.04, 1.76, 5.13, and 1.66 μM , respectively. Therefore, 1,2,3-triazole-pyridine hybrid might be a promising scaffold to develop antitumor agents against esophageal cancer.

3.3. 1,2,3-Triazole-pyridine hybrids were novel FTO inhibitors

Because of potent antiproliferative activity against all esophageal cancer cell lines, compound **C6** and **C8** were selected to evaluate their inhibitory activity against FTO. From the results of enzymatic inhibitory activity in Figure 2(A,B), compound **C6** and **C8**, respectively, displayed the potent inhibitory effects against FTO with IC_{50} values of 780 and 8670 nM. These results indicated that 1,2,3-Triazole-pyridine hybrids might be potential FTO inhibitors.

Recent references showed that FTO is aberrantly upregulated in various cancers, and down-regulation of LSD1 by RNAi or pharmacological inhibition has been an effective strategy to suppress the development of various cancer¹⁶. In this work, EC109&shFTO (FTO knock-down cells) and EC109&shControl (control cells) cell lines were cultured to investigate the *in vitro* antiproliferative activity of FTO inhibitors. Firstly, the expression of FTO in EC109&shFTO and EC109&shControl cells was detected and the results are shown in Figure 2(C). Then, MTT assay was performed to examine the antiproliferative activity of FTO inhibitor **C6**. From the results of Figure 2(D), FTO inhibitor **C6** exhibited inhibitory effects with an IC_{50} value of 1.06 μM against EC109&shControl cells. In contrast, compound **C6** inhibited EC109&shFTO cells with an IC_{50} value of 3.97 μM , about 3–4 fold less potent against EC109&shControl cells. The activity discrepancy in Figure 2(D) demonstrated that antiproliferative effects of

compound **C6** against EC109 cells had a relationship with the FTO inhibition.

3.4. Molecular docking of FTO inhibitors

Due to different inhibitory effects of 1,2,3-Triazole-pyridine hybrids **C6** and **C8** against FTO, their molecular docking studies were investigated in this work. To predict the binding models between compounds and FTO, docking analysis using the Autodock software was performed. PDB code was 5DAB and FTO protein was downloaded from the RCSB protein database. As shown in Figure 3, compound **C8** locates into the active pocket of FTO and forms the hydrogen-bond interaction with Lys107, Leu109, and Asn235. As a reference molecule, FB23-2 was also docked using the same methods. From the results in Figure 3(D), FB23-2 as a reported FTO inhibitor (yellow structure) was docked into a similar pocket as compound **C8**.

As shown in Figure 4, compound **C6** was docked into the active site of FTO and displayed the potent inhibitory activity against FTO. The amide group attaching to 1,2,3,4,5-pentafluorobenzene ring of 1,2,3-Triazole-pyridine hybrid **C6** formed a hydrogen bond with Lys107. 1,2,3-Triazole unit of compound **C6** formed two hydrogen bonds with Lys107 and Asn110 of FTO. In addition, pyridine unit of compound **C6** also formed two hydrogen bonds with Tyr108 and Leu109 of FTO. From the results in Figure 4(D), FB23-2 as a reported FTO inhibitor (red structure) was docked into a similar pocket as compound **C6**.

3.5. Cell cycle analysis

N^6 -Methyladenosine ($m^6\text{A}$) modification is the major chemical modification in mRNA that controls cell proliferation and cell cycle¹⁷. Recent studies reported that FTO demethylates *Cyclin D1* mRNA and controls cell cycle progression¹⁸. In order to explore

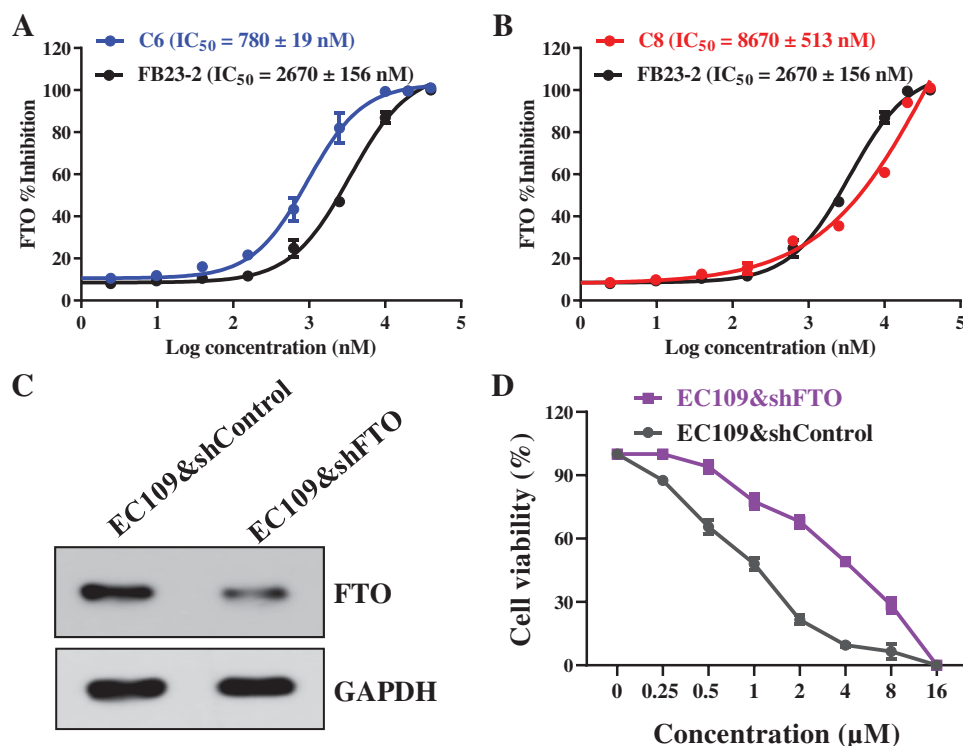


Figure 2. 1,2,3-Triazole-pyridine hybrids were novel FTO inhibitors. (A) The inhibitory activity of compound **C6** against FTO; (B) The inhibitory activity of compound **C8** against FTO; (C) Expression of FTO in EC109&shFTO and EC109&shControl cells; (D) Cell viability of compound **C6** against EC109&shFTO and EC109&shControl cells. FB23-2 as a reported FTO inhibitor was the reference molecule.

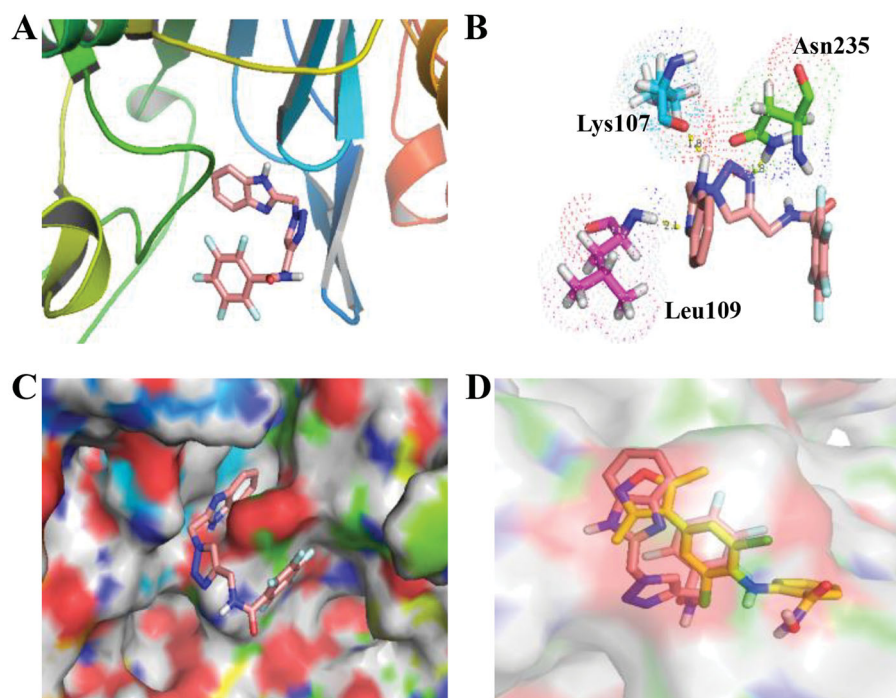


Figure 3. Molecular docking of compound **C8** (PDB code: 5DAB). (A) Compound **C8** binds to subunits of FTO; (B) Hydrogen-bond interaction of compound **C8** and FTO; (C) Compound **C8** locates into the active pocket of FTO; (D) a similar pocket between FB23-2 (yellow structure) and compound **C8**.

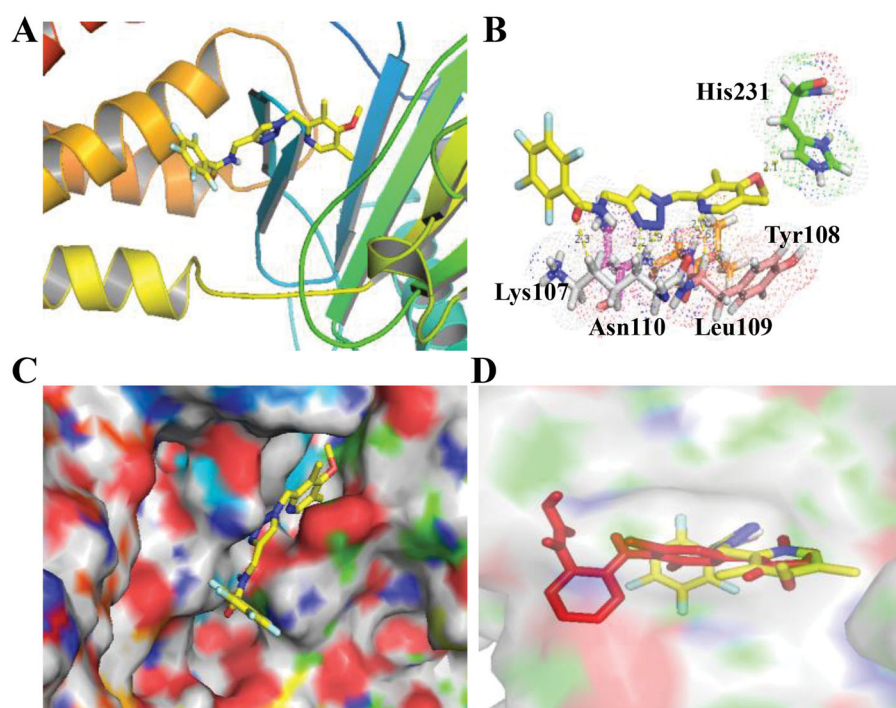


Figure 4. Molecular docking of compound **C6** (PDB code: 5DAB). (A) Compound **C6** binds to subunits of FTO; (B) Hydrogen-bond interaction of compound **C6** and FTO; (C) Compound **C6** locates into the active pocket of FTO; (D) a similar pocket between FB23-2 (red structure) and compound **C6**.

the effects of cell cycle of compound **C6**, TE-1 and EC109 cell lines were selected according to its antiproliferative activity results. From the cell cycle analysis of compound **C6** at different concentrations against TE-1 and EC109 cells in Figure 5(A), it arrested cell cycle at G2 phase accompanying with the decrease of cells at G1 and S phase in a concentration-dependent manner. These findings indicated that compound **C6** as a novel FTO inhibitor could arrest cell cycle against esophageal cancer.

3.6. The regulation of epithelial mesenchymal transition (EMT) pathway

Epithelial mesenchymal transition (EMT) as a critical cellular programme in which epithelial cells undergo series of biochemical changes to acquire mesenchymal phenotype displays important roles in the development of esophageal cancer¹⁹. EMT is characterised by the upregulation of N-cadherin and the downregulation of E-cadherin, which is regulated by a complex network of signalling

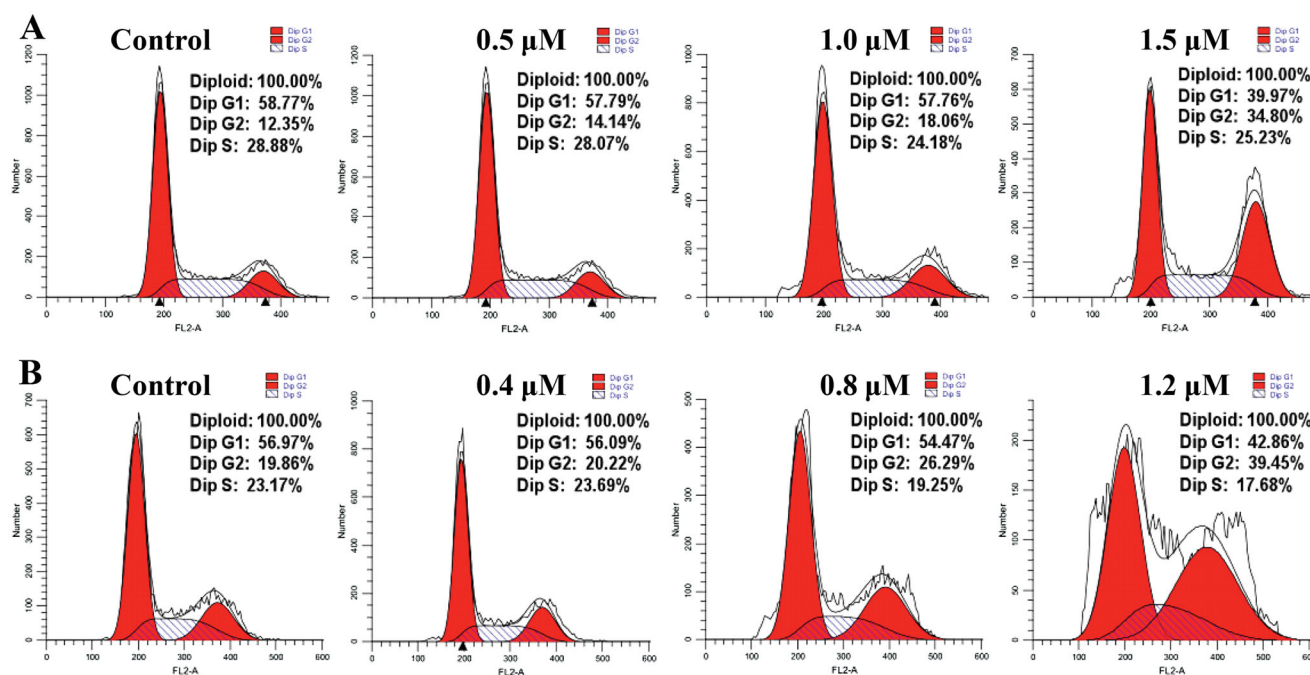


Figure 5. Cell cycle analysis of compound **C6** against TE-1 (A) and EC109 (B) cells.

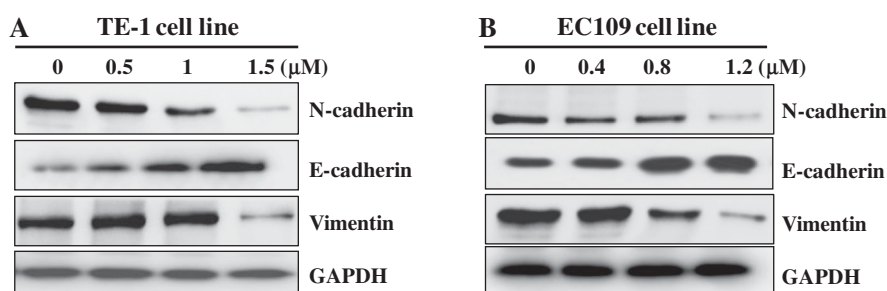


Figure 6. Compound **C6** regulated EMT pathway against TE-1 (A) and EC109 (B) cells.

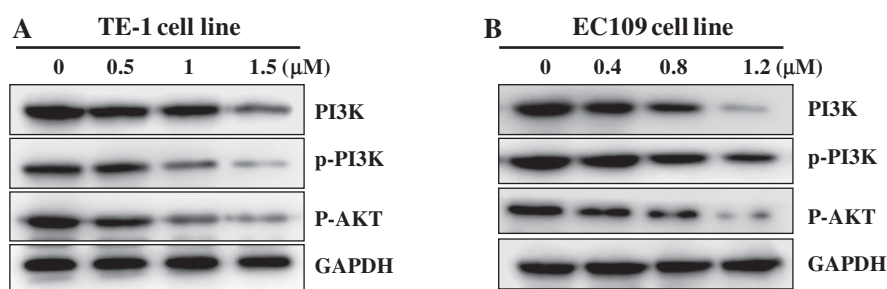


Figure 7. Compound **C6** regulated PI3K/AKT pathway against TE-1 (A) and EC109 (B) cells.

pathways and transcription factors²⁰. To further explore the anti-cancer mechanism of FTO inhibitor **C6**, TE-1, and EC109 cell lines were treated for 48 h. From the results in Figure 6, the expression levels of N-cadherin and Vimentin were decreased and the expression level of E-cadherin was increased against TE-1 and EC109 cells in a concentration-dependent manner, demonstrating that FTO inhibitor **C6** could inhibit EMT pathway against esophageal cancer.

3.7. The regulation of PI3K/AKT pathway

Dysregulation of FTO was implicated in multiple biological processes including proliferation and cell cycle against different tumors²¹. Importantly, these modulations might rely on the communications between FTO and PI3K/AKT signalling pathway²². In

recent years, studies have shown that components of the PI3K/AKT signalling pathway are frequently altered in esophageal cancer²³. TE-1 and EC109 cell lines were treated with FTO inhibitor **C6** at different concentrations for 48 h to perform western blot. From the results in Figure 7, the expression levels of PI3K, p-PI3K, and p-AKT were decreased against TE-1 and EC109 cells in a concentration-dependent manner, indicating that FTO inhibitor **C6** could regulate PI3K/AKT pathway against esophageal cancer.

3.8. In vivo antitumor study

Due to the potent inhibitory activity of FTO inhibitor **C6** against esophageal cancer EC109 cell line, we also evaluated the *in vivo* anticancer effects of FTO inhibitor **C6** on xenograft models

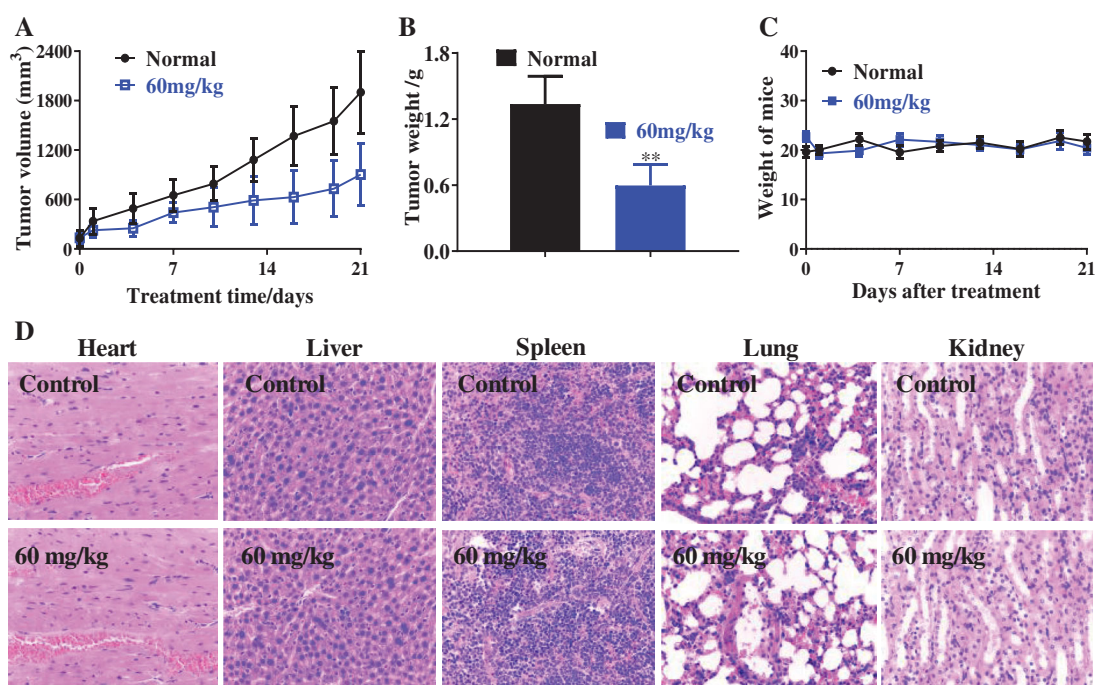


Figure 8. *In vivo* antitumor effects of compound **C6**. (A) Tumour volume; (B) Tumour weight; (C) Weight of mice; (D) Haematoxylin and eosin staining. $**p < 0.01$.

bearing EC109 cells. After the treatment of FTO inhibitor **C6** with the dose of 60 mg/kg, the tumour weight, the weight of mice and tumour volume were measured and recorded. From the results in Figure 8(A,B), FTO inhibitor **C6** inhibited tumour growth in esophageal cancer xenograft models remarkably. Weight of mice was almost unchanged in Figure 8(C) demonstrating that FTO inhibitor **C6** displayed the potent anticancer effects without obvious toxicities. In addition, main organs (Heart, liver, spleen, lung, and kidney) of oesophageal cancer xenograft models were performed haematoxylin and eosin staining. As shown in Figure 8(D), these results also suggested low global toxicities.

4. Conclusions

In summary, a novel series of 1,2,3-triazole-pyridine derivatives were synthesised according to click reaction and further evaluated for their inhibitory activity against five esophageal cancer cell lines (KYSE-150, KYSE-270, TE-1, KYSE-510, and EC109). Among them, compound **C6** displayed the most potent antiproliferative activity against KYSE-150, KYSE-270, TE-1, KYSE-510, and EC109 cell lines with IC_{50} value of 2.17, 1.35, 0.95, 4.15, and 0.83 μ M, respectively. In this work, compound **C6** was identified as a novel FTO inhibitor and regulated EMT pathway and PI3K/AKT pathway against esophageal cancer. Importantly, *In vivo* antitumor effects of compound **C6** showed that it was an orally anticancer agent with potent effects and low toxicities. Therefore, FTO might be a potential therapeutic target in esophageal cancer, and compound **C6** could be a promising candidate for the drug discovery to treat esophageal cancer.

Disclosure statement

No potential conflict of interest was reported by authors.

Funding

This research was supported by National Natural Science Foundation of China [No. 31900502] and The Youth Talent Lifting Project of Henan Province [No. 2021HYTP044].

References

- Bollschweiler E, Plum P, Mönig SP, et al. Current and future treatment options for esophageal cancer in the elderly. *Expert Opin Pharmacother* 2017;18:1001–10.
- Huang FL, Yu SJ. Esophageal cancer: risk factors, genetic association, and treatment. *Asian J Surg* 2018;41:210–5.
- Qin B, Dong M, Wang Z, et al. Long non-coding RNA CASC15 facilitates esophageal squamous cell carcinoma tumorigenesis via decreasing SIM2 stability via FTO-mediated demethylation. *Oncol Rep* 2021;45:1059–71.
- Cui Y, Zhang C, Ma S, et al. RNA m6A demethylase FTO-mediated epigenetic up-regulation of LINC00022 promotes tumorigenesis in esophageal squamous cell carcinoma. *J Exp Clin Cancer Res* 2021;40:294.
- Liu S, Huang M, Chen Z, et al. FTO promotes cell proliferation and migration in esophageal squamous cell carcinoma through up-regulation of MMP13. *Exp Cell Res* 2020;389:111894.
- Dobie C, Montgomery AP, Szabo R, et al. Synthesis and biological evaluation of selective phosphonate-bearing 1,2,3-triazole-linked sialyltransferase inhibitors. *RSC Med Chem* 2021;12:1680–9.
- Srivastava A, Aggarwal L, Jain N. One-pot sequential alkynylation and cycloaddition: regioselective construction and biological evaluation of novel benzoxazole-triazole derivatives. *ACS Comb Sci* 2015;17:39–48.
- Ashwini N, Garg M, Mohan CD, et al. Synthesis of 1,2-benzoxazole tethered 1,2,3-triazoles that exhibit anticancer activity in acute myeloid leukemia cell lines by inhibiting

- histone deacetylases, and inducing p21 and tubulin acetylation. *Bioorg Med Chem* **2015**;23:6157–65.
- Humphries-Bickley T, Castillo-Pichardo L, Hernandez-O'Farrill E, et al. Characterization of a dual Rac/Cdc42 inhibitor MBQ-167 in metastatic cancer. *Mol Cancer Ther* **2017**;16:805–18.
 - Sahu R, Mishra R, Kumar R, et al. Pyridine moiety: an insight into recent advances in the treatment of cancer. *Mini Rev Med Chem* **2022**;22:248–72.
 - Prakash M, Itoh Y, Fujiwara Y, et al. Identification of potent and selective inhibitors of fat mass obesity-associated protein using a fragment-merging approach. *J Med Chem* **2021**;64:15810–24.
 - Shishodia S, Demetriades M, Zhang D, et al. Structure-based design of selective fat mass and obesity associated protein (FTO) inhibitors. *J Med Chem* **2021**;64:16609–25.
 - Xu Z, Zhao SJ, Liu Y. 1,2,3-Triazole-containing hybrids as potential anticancer agents: current developments, action mechanisms and structure-activity relationships. *Eur J Med Chem* **2019**;183:111700.
 - Haranahalli K, Honda T, Ojima I. Recent progress in the strategic incorporation of fluorine into medicinally active compounds. *J Fluor Chem* **2019**;217:29–40.
 - Fu DJ, Liu YC, Yang JJ, et al. Design and synthesis of sulfonamide-1,2,3-triazole derivatives bearing a dithiocarbamate moiety as antiproliferative agents. *J Chem Res* **2017**;41:523–5.
 - Zhou LL, Xu H, Huang Y, et al. Targeting the RNA demethylase FTO for cancer therapy. *RSC Chem Bio* **2021**;2:1352–69.
 - Hirayama M, Wei FY, Chujo T, et al. FTO demethylates Cyclin D1 mRNA and controls cell-cycle progression. *Cell Rep* **2020**;31:107464.
 - Wu R, Liu Y, Yao Y, et al. FTO regulates adipogenesis by controlling cell cycle progression via m6A-YTHDF2 dependent mechanism. *Biochim Biophys Acta Mol Cell Biol Lipids* **2018**;1863:1323–30.
 - Tang Q, Lento A, Suzuki K, et al. Rab11-FIP1 mediates epithelial-mesenchymal transition and invasion in esophageal cancer. *EMBO Rep* **2021**;22:e48351.
 - Loh CY, Chai JY, Tang TF, et al. The E-cadherin and N-cadherin switch in epithelial-to-mesenchymal transition: signaling, therapeutic implications, and challenges. *Cells* **2019**;8:1118.
 - Zhang C, Zhang M, Ge S, et al. Reduced m6A modification predicts malignant phenotypes and augmented Wnt/PI3K-Akt signaling in gastric cancer. *Cancer Med* **2019**;8:4766–81.
 - Liu Y, Wang R, Zhang L, et al. The lipid metabolism gene FTO influences breast cancer cell energy metabolism via the PI3K/AKT signaling pathway. *Oncol Lett* **2017**;13:4685–90.
 - Zhang L, Tong Z, Sun Z, et al. MiR-25-3p targets PTEN to regulate the migration, invasion, and apoptosis of esophageal cancer cells via the PI3K/AKT pathway. *Biosci Rep* **2020**;40:BSR20201901.